Proceedings of ICFDP7:
The Seventh International Congress on Fluid Mechanics
December 18-20, 2001, Cairo, Egypt

ICFDP7-2001064

SIMULATION OF THE CONTROL OF FLOW SEPARATION USING SYNTHETIC JETS

Dr. G. Simandirakis
Research Assistant
Thermal Turbomachinery Lab.
National Technical University of Athens, Greece
gsiman@ltt.ntua.gr

Prof. K.D. Papailiou
Professor
Head of Thermal Turbomachinery Lab.
National Technical University of Athens, Greece
kpapail@ltt.ntua.gr, Fax: +30-1-7721658

ABSTRACT

It has been known from experiments for years, that flow separation can be controlled using pulsating jets while spending small amounts of energy. It seems that the unsteady vorticity created by the pulsating jet, activates flow instabilities, which result in moving parts of the flow towards the low energy material in the separated regions. The net result is that flow separation is partly or totally eliminated.

Positioning the jets and specifying their frequency and amplitude requires a computational tool, which must be affordable for practical situations.

Such a tool, based on two equation models for describing the turbulence behavior is presented in this paper. Comparisons with experimental results are also presented, which are discussed, in order to conclude on the physical aspects of this important flow control mechanism.

NOMENCLATURE

c_μ	steady blowing momentum coefficient, ($\equiv J/cq$) oscillatory blowing momentum coefficient, ($\equiv J'/cq$)
c	model reference chord
c_p	wall pressure coefficient, ($\equiv (P-Ps)/q$)
f	excitation frequency
F^+	reduced frequency, ($\equiv (f*x_{sep})/ U_\infty$)
J	jet momentum at slot exit
J′	RMS value of fluctuating jet momentum at slot exit
q	free steam dynamic pressure, ($\equiv 1/2\rho U_\infty^2$)
Rc	chord Reynolds number, ($\equiv U_\infty c/\nu$)
x/c	dimensionless steam-wise location
x_{sep}	distance from separation to reattachment
U_∞	average velocity at free–stream conditions
ν	kinematic viscosity
ρ	density

INTRODUCTION

Flow separation traditionally has been controlled utilizing suction or blowing appropriately applied. It has been demonstrated, however, that this flow control approach results in heavy losses of useful energy, so that the resulting gain is not always cost effective. Investigations, which were realized during the last thirty years demonstrated, however, that the same effect could be achieved, as demonstrated by experiments, by means of energy expense two or three orders of magnitude below that required by the flow control mechanisms described above. These investigations, the quasi-totality of them experimental, demonstrated that unsteady flow perturbations (jets) in regions where they could be amplified, resulted in a drastic reorganization of the flow structure with, as a consequence, the reenergetization of the low energy areas of the flow. The net result was that areas of separation disappeared, party or wholly, with obvious benefits for the flow behavior.

In order to exploit this flow control approach, research was directed towards understanding the physical phenomena, which are not even now well understood, developing the excitation mechanical devices, which should be quite small, and developing appropriate prediction tools. Understanding is progressing slowly, both because the corresponding stability analysis for such a flow situation has not yet been established, and because Direct Numerical Simulation (DNS) was, up to now, assumed to be the only numerical approach producing useful information.

Micro electromechanical devices (MEMS), which have the right size and could be used to exit the flow at the required frequency, seem to be manufacturable now, but a faster computational method, which would be reproducing reality using adequate modeling, remains still to be established. The potential benefits of this flow control approach are very important, as it may be easily seen.

The authors decided to investigate the assumption that the pulsating (or synthetic) jet influence was introduced to the flow though its mean vorticity, which could be well established through computations using simple turbulence models.

For this reason, a 2D accurate and sensitive unsteady method, developed at LTT/NTUA, was used, in which simple turbulence

models (Baldwin Lomax corrected for blowing/suction conditions and Launder – Sharma k-ε) were implemented.

NAVIER-STOKES CODE

The Navier-Stokes solver employed, is an explicit, time-marching fractional-step solver for the calculation of two-dimensional, steady and unsteady compressible flows embodying some modifications to treat the control and the interaction region. In the present method the conservative two-dimensional Navier-Stokes equations are split in a sequence of one-dimensional operators for the inviscid part, the viscous part and the source terms. Thus, instead of applying a pure two-dimensional scheme, a number of one-dimensional steps are executed for which numerical stability constraints are less strict.

The corresponding unsteady Favre-averaged Navier-Stokes equations, with a low-Reynolds k-ε closure, are transformed to the body-fitted coordinate system defined by the grid lines of the grid generated. In the computational plane (ξ,η) the resulting equations may be cast in the following conservative form.

$$\frac{\partial \vec{Q}}{\partial t}+\frac{\partial \vec{F}}{\partial \xi}+\frac{\partial \vec{G}}{\partial \eta}=\vec{S} \qquad (1)$$

According to the fractional-step concept, the time evolution of the unknown vector array Q is obtained by applying the sequence of operators, which may be cast in the following symbolic form

$$\vec{Q}^{n+2} = L_\xi^H L_\eta^H L_\xi^P L_\eta^P L^{ST} L^{ST} L_\eta^P L_\xi^P L_\eta^H L_\xi^H \vec{Q}^n \qquad (2)$$

A double and inverse sequence of the one-dimensional operators leads to a second order accuracy in time, while the calculated quantities have a physical meaning only at the end of a 2Δt time interval (i.e., going from the n, to n+2 iteration level), Abarbanel and Gottlieb[12]. With regard to the treatment of the source terms, a semi-implicit scheme is used to ensure numerical stability. Thus, for the solution of the intermediate step, the following equation provides the L^{ST} operator,

$$\frac{\partial \vec{Q}}{\partial t} = \vec{S} \qquad (3)$$

The right-hand-side array S splits in S_+, which contains the positive source terms, and S. containing the negative ones. The negative part is Newton-linearized and the delta form of Equation (3) is written as

$$\left[I - \Delta t^* \cdot \left(\frac{\partial \vec{S}_-}{\partial \vec{Q}} \right)^{n+\frac{4}{5}} \right] \Delta \vec{Q}^{n+\frac{4}{5}} = \Delta t^* \cdot \vec{S}^{n+\frac{4}{5}} \qquad (4)$$

Extra dissipation terms are explicitly added, Simandirakis[13], to the solution array. Q at the end of a complete calculation period, corresponding to a time interval of 2Δt, may be written as follows

$$\vec{Q}^{n+2} = \vec{Q}^{n+2} + \vec{D}_\xi + \vec{D}_\eta \qquad (5)$$

In the context of the present work, in order to incorporate in the solver a control mechanism and since the flow is fully turbulent in the jet-flow boundary layer interaction zone, necessary modifications were performed in the solver (wall boundary conditions, turbulence modelling) in order to account for wall suction or blowing.

Turbulence modelling

The Baldwin-Lomax model is applied following the two-layer approach. Nevertheless, important modifications are introduced concerning (a) the calculation of the wall shear stress close to the separation point, (b) the calculation of the maximum of the function F(y) when the latter displays two peaks and (c) the prediction of transition.

According to Chen [9] and Bur [10], the main influence of the mass injection through the porous surface in the control region is restricted to the portion of the boundary layer very close to the wall. Also, as many authors suggest, it is preferable to treat this zone with a robust turbulence model such as the algebraic Baldwin-Lomax model. In the case that a more elaborate turbulence model is used, such as the k-ε model (already incorporated in the code), it is proposed to maintain it for the outer part of the boundary layer and switch to an algebraic one for the inner zone.

Having analysed the problem that transpiration effects have to be taken into account in the turbulence modelling, numerous modifications for the Van Driest wall damping function have been proposed in the literature (Cebeci, Kinney and Sparrow, Chen, Rotta). In the present study the extension proposed by Cebeci [15] is incorporated. Consequently, the Van Driest wall damping function is generalized for the simultaneous presence of mass transfer through the wall and a longitudinal pressure gradient.

Hence, the damping function D as used in the vicinity of solid walls is now given by

$$D = 1 - \exp\left(- \frac{y^+}{A^+} \right) \qquad (6)$$

where

$$A^+ = 26 \left\{ (11.8 Up^+) - \frac{p^+}{U\, p^+} \left[\exp(11.8 U\, p^+) - 1 \right] \right\}^{-1/2} \qquad (7)$$

and

$$Up^+ = \frac{Up}{u_\tau} \quad , \quad p^+ = - \frac{v}{\rho\, u_\tau^3} \frac{dp}{ds} \qquad (8)$$

RESULTS

First a numerical test case was arranged, investigating the capabilities of our CFD software in reproducing the experimentally observed positive action of blowing-suction devices just ahead of separation outbreak situations.

The run concerns the internal 2D flow inside a symmetric straight channel with a ramp (Figure 1). The resulting nozzle-shaped geometry causes the flow to separate just after the broadening of the area, depending on the flow Reynolds number. At first, steady state flow conditions were tested varying the Reynolds number of the flow between 100,000 and 1,000,000, and using both Baldwin-Lomax, and low Reynolds k-å turbulent models. The extension of the separation region after the ramp depended on the Reynolds number of the flow.

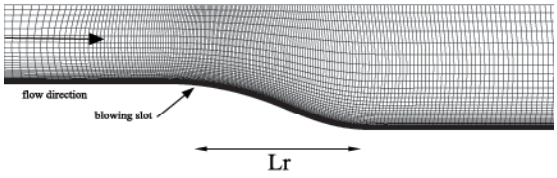

Figure 1: Grid of half channel geometry of the numerical test.

Afterwards, a laminar like run was attempted, observing the behavior of the flow field, initializing a "control" mechanism. The "control" mechanism consists of a momentum-supplying surface forth and below the separation-issuing region. The control surface may comprise a thin porous plate through which blowing and suction is accommodated to the main flow, or a vibrating metal panel. The distribution of the normal to the wall velocity component along the slot obeys the law described in reference [1],

$$v(s) = v_w A\cos(2\pi ft) \qquad (9)$$

where, A is the forcing amplitude and f the frequency.

The flow was compressible and entered the channel at zero angle, at a velocity U_∞ = 150 m/s. The Reynolds number on the channel length was equal to 500,000, the blowing-suction slot was placed just ahead of the broadening area, and the total length of the “bump” was L_r = 0.042 m. A forcing frequency f = 20,000 Hz was used, and a forcing amplitude A = 5%. The above gave a reduced frequency value equal to

$$F^+ = \frac{f \cdot L_r}{U_\infty} = 5.33 \qquad (10)$$

The reduced frequency F^+ must have a value greater than 1. Otherwise the periodic excitation introduced by the triggering mechanism just ahead of the separation region, cannot affect the mean flow, Wygnaski [3,4]. Special care was taken to account for the vortices exiting the outflow boundary. The disturbances must pass through this boundary without causing reflections that would affect the upstream flow. So, near the outflow boundary, a buffer domain technique was introduced to the solver [2].

A first run was carried out without triggering the flow field through the slot, and a second using the aforementioned triggering mechanism. For both runs, the resulting flow fields of vorticity are shown in figure (2). Observing the flow field, two completely different structures of vortices emanating from the beginning of the ramp are clearly seen. In the "control" case, the vortices are significantly smaller, and have the tendency to stay attached to the wall as they travel downstream.

It seems that the forced frequency, introduced in the flow field, has altered the flow structure. In figure (3) the RMS value of the stream-wise component of the velocity fluctuations over the boundary layer, integrated in time, $\langle c_m \rangle$ is shown near the ramp region. The $\langle c_m \rangle$ value is defined by the following equation

$$\langle c_m \rangle = \frac{2}{U_i^2 L_F} \int_0^\delta < u' >^2 dy \qquad (3)$$

It can be seen from figure (3) that the velocity fluctuations in the region after the control is applied (the extend of which is indicated by the arrow) are visibly decreased.

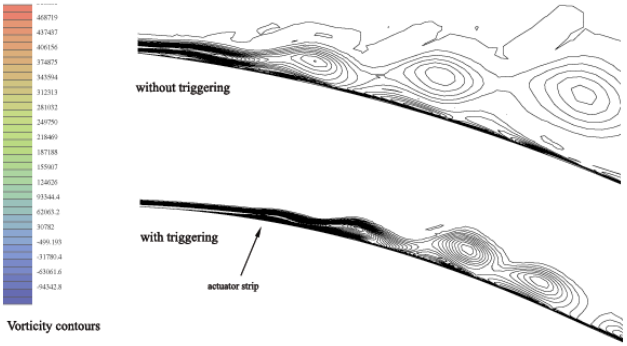

Figure 2: Vorticity contours.

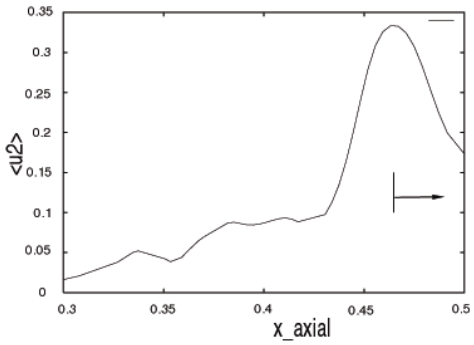

Figure 3: Time integration of the RMS velocity fluctuations near the ramp region.

This method was also used in order to analyze the data produced by Avi Seifert and La Tunia G. Pock on the lower wall of a channel with a bump, which was simulating a profile suction side [5]. Flow separation was present in the rear part of the bump.

The test case concerns the flow though a channel with a rectangular cross section. The upper wall is straight while along the lower one, a bump exists which simulates the upper surface of a 20% thick airfoil at zero angle of attack. Detailed geometry may be found in [5]. In the experiment, the bump reference chord was 200 mm. The location of the airfoil leading edge was at x/c=0. Also two alternative blowing slots were available at x/c=0.59, and x/c=0.64. In the present study only the second case is examined. The slots were about 0.25% chord wide (0.50 mm). The slots were inclined at 30° to the surface (injection angle was 30° facing downstream from the wall tangent direction). A picture of the geometry is shown in figure (4). The computation domain extends 1 chord upstream of the airfoil shaped bump and 1.2 chords downstream.

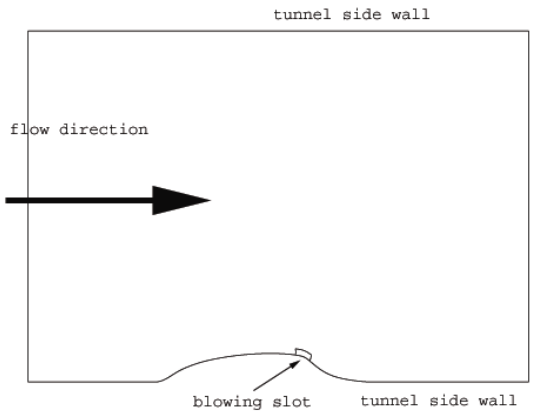

Figure 4: Geometry of the experiment tunnel (0.33m by 0.33m cross section).

The computations in this case were fully turbulent. Both the Baldwin-Lomax algebraic model and the k-ε two equations model were used. The flow exhibits a mild favorable pressure gradient until x/c = 0.55. Without control the flow separates at the slope discontinuity present at x/c ≅ 0.66. The situation described is quite different from a real airfoil case, because, due to the tunnel walls, there is a reattachment of the flow downstream of the "airfoil".

In order to simulate the region above the narrow slot, a multi-block strategy was used. The chosen method was that of the overlapping sub-grids, for greater flexibility in the grid construction. The connection between the grids was obtained by interpolation [8]. The stretching of the grid lines for the second grid was around the position of the slot, at x/c=0.64. A close-up picture on this region is presented in figure (5).

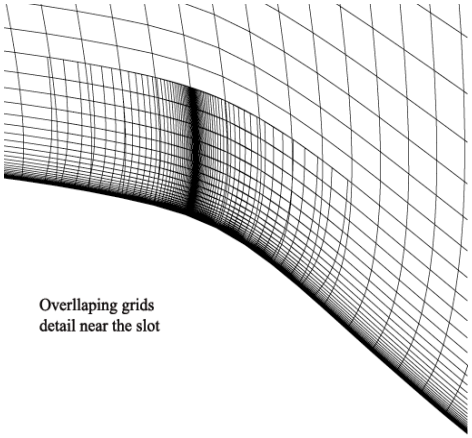

Figure 5: Grids detail at the slot area near the wall.

In figure (6), streamlines of the flow field together with the velocity vectors are shown, presenting instantaneous flow emanating from the slot and entering the tunnel.

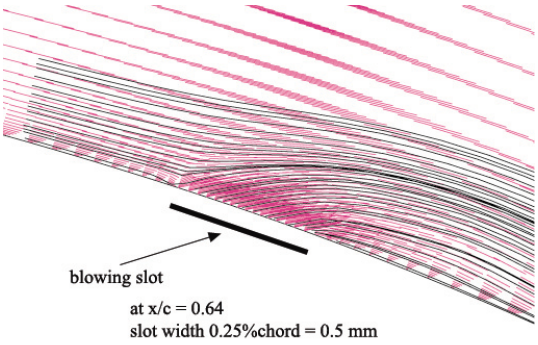

Figure 6: Detail of the flow field, streamlines and velocity vectors near the blowing slot.

Comparisons of theoretical and experimental results are presented in figures (7), (8) and (9). In all figures, the comparison is made in a respect to the location of the bump, the shape of which is present in all three figures.

Figure (7) presents the comparison of theoretical results with experiment, when no control is applied. The Reynolds number based on chord is equal to $7x10^6$. The Mach number of the main flow was equal to 0.25. Separation is present and no pressure recuperation is experienced (note that for Cp a reversed ordinate scale is used). The agreement between theory and experiment may be termed satisfactory.

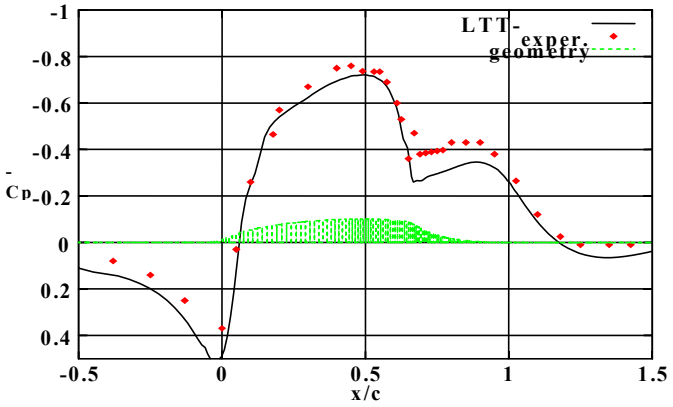

Figure 7: Comparison between theory and experiment. No flow control case. This figure corresponds to Fig. 10 of ref. (5). Calculation using the Launder Sharma k-ε model.

Next, in figure (8), comparisons are presented of theoretical and experimental results, for the case of flow control through continuous steady suction of 4%, that is

$$c_\mu = \frac{J}{cq} = 4\% \qquad (11)$$

Again, the agreement between theory and experiment may be termed satisfactory.

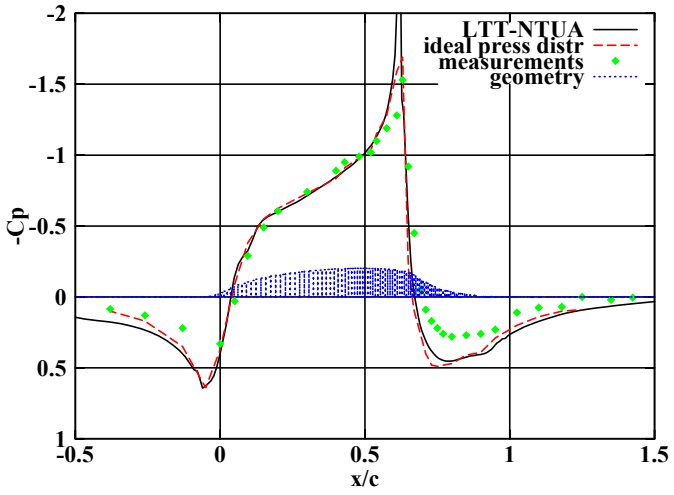

Figure 8: Comparison between theory and experiment. Application of flow control (4% suction). This figure corresponds to Fig. 11 of ref. (5). Calculation was done using the Launder Sharma k-ε model.

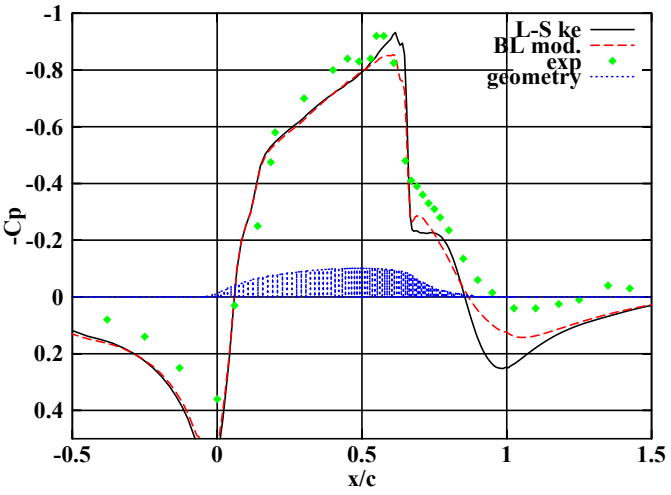

Figure 9: Comparison between theory and experiment. Application of synthetic jet with characteristics F^+ =1.15, c_μ=0.16%.

This figure corresponds to Fig. 12 of ref. (5). Calculation using the Launder Sharma k-ε and the Baldwin-Lomax (corrected for suction/blowing effects) models was performed.

Finally, in Figure (9), comparisons are presented between theoretical and experimental results for a case, where a synthetic jet (only oscillating component in this case) is present, with a reduced frequency of

$$F^+ = \frac{f \cdot x_{sep}}{U_\infty} = 1.15 \qquad (12)$$

and a reduced amplitude of the oscillatory blowing momentum coefficient equal to

$$\left\langle C_\mu \right\rangle = \frac{\left\langle J' \right\rangle}{\left\langle c \cdot q \right\rangle} = 0.16\% \qquad (13)$$

where, f is the excitation frequency, x_{sep} is distance from separation to reattachment of the flow U_∞ is the average velocity at free–stream conditions, J′ is the RMS value of the fluctuating jet momentum at the slot exit, c is the model reference chord, and q is the free steam dynamic pressure.

Both k-ε and Baldwin-Lomax models were used for the computations. It can be seen that, again, the agreement between theory and experiment may be termed satisfactory.

It can also be seen that the pressure recuperation is not as complete as for the continuous suction case. However, it is quite important, particularly in view of the amount of energy that was provided, in order to obtain this result.

Conclusions

The main conclusion of the paper is that the comparisons between theory and experiments suggest that it is possible to provide information concerning the position, amplitude and frequency of pulsating jets, when flow separation control is required through pulsating (synthetic) jets, by means of simple turbulence models and time averaged mean turbulent flow computations. This fact becomes important, when complex flows are examined, where both flow separation location and "testing" have to be performed through affordable computations, in order to be able to find a realistic solution with this kind of flow control. The computations indicate that pressure recovery may only be partial and the corresponding flow is marked by moving flow vortices. These computations suggest, as well, that mean flow vorticity is the key element underlying this very important kind of active control. Additional work is, however, needed in order to assess beyond all reasonable doubt the statements made above.

ACKNOWLEDGMENTS

The results of this paper were obtained during the project Aeromems, funded by the European Commission in the Aeronautics Program (contract BRPR-CT97-0573). The authors would like to thank the European Commission for its help and their partners for their continuous encouragement.

REFERENCES

1. H. L. Zhang and H.F. Fasel, "Numerical Investigation of the evolution and control of two-dimensional unsteady separated flow over a Stratford ramp" AIAA paper 99-1003, 37th

AIAA Aerospace Sciences Meeting and Exhibit, Reno, NV, January 1999
2. M. Kloker and U. Konzelmann "Outflow Boundary Conditions for Spatial Navier-Stokes Simulations of Transition Boundary Layers" AIAA Journal, Vol. 31, No. 4, April 1993.
3. Wygnanski I., “Boundary Layer and Flow Control by Periodic Addition of Momentum (Invited)”, AIAA paper 97-2117, 4th AIAA Shear Flow Control Conference, Silvertee Hotel, Snowmass Village, CO, June 1997.
4. Gaster M., Kit E., Wygnanski I., “Large-scale structures in a forced turbulent mixing layer” J. Fluid Mech. (1985), vol. 150, pp. 23-39.
5. Avi Seifert and LaTunia G. Pack "Active Control of Separated Flows on Generic Configurations at High Reynolds Numbers", AIAA paper 99-3403, 30th AIAA Fluid Dynamics Conference, Norfolk, VA, June 1999.
6. LaTunia G. Pack and Avi Seifert "Dynamics od Active Separation Control at High Reynolds Numbers", AIAA paper 2000-0409, 38th AIAA Aerospace Sciences Meeting and Exhibit, Reno, NV, January 2000.
7. Avi Seifert and LaTunia G. Pack "Sweep and Compressibility Effects on Active Separation Control at High Reynolds Numbers", AIAA paper 2000-0410, 38th AIAA Aerospace Sciences Meeting and Exhibit, Reno, NV, January 2000.
8. Wehr Dieter, Stangl Roland, Wagner Siegfried, "Interpolation Schemes for Intergrid Boundary Value Transfer applied to Unsteady Transonic Flow Computations on Overlaid Embedded Grids", Computation Fluid Dynamics 94, pp 383-389.
9. Chung-Lung Chen, Chuen-Uen Chow et al., "Computation of Viscous Transonic Flow over Porous Airfoils", Paper AIAA-87-0359, 1987.
10. Bur R., "Etude Fondamentale sur le Controle Passif de l'Interaction onde de Choc/Couche Limite Turbulente en Ecoulement Transsonique", Thése de Doctorat de l'universitè Paris 6, 1992.
11. Bur R., "Passive Control of a Shock Wave/Turbulent Boundary Layer Interaction in a Transonic Flow", Rech Aérosp. no 1992-6.
12. Abarbanel S., Gottlieb D., "Optimal Time Splitting for Two- and Three-Dimensional Navier-Stokes Equations with Mixed Derivatives", Journal of Computational Physics 41, 1981.
13. Simandirakis G., "Numerical Solutions of Navier-Stokes Equations for Transonic Flows Inside Turbine Bladings", Ph.D. Thesis, Athens, February 1992.
14. Simandirakis G., Dejean F., Vassilopoulos Ch., Giannakoglou K., Papailiou K.D., "Steady and Unsteady Two-Dimensional Flow Calculations Using an Explicit Fractional-Step Algorithm", Proc. of the ECCOMAS 94 Conference, 5-8 September, Stuttgart, Germany, pp. 701-710.
15. Cebeci T., Smith A.M.O., "Analysis of Turbulence Boundary Layers", Academic Press, London, 1974.
16. Van Driest E.R., "Turbulent Boundary Layers in Compressible Fluids", J. Aero Sciences, Vol. 18, (1951).
17. Le Balleur J.C., "Calcus Couplés Visqueux-Non Visqueux, Incluant Decollements et Ondes de Choc en Ecoulement Bidimensionnel, AGARD LS-94, (1978).